Microchemical Journal 153 (2020) 104325

Contents lists available at ScienceDirect

Microchemical Journal

journal homepage: www.elsevier.com/locate/microc

Antifungal efficiency of individual compounds and evaluation of non-linear effects by recombining fractionated turpentine

Joel Ljunggren[a,*], Dan Bylund[b], Bengt Gunnar Jonsson[b], Mattias Edman[b], Erik Hedenström[a]

[a] Department of Chemical Engineering, Mid Sweden University, Sweden
[b] Department of Natural Sciences, Mid Sweden University, Sweden

ARTICLE INFO

Keywords:
Turpentine composition
Bioassay
Coniophora puteana
Growth inhibition
Fractions
Synergism
Antagonism

ABSTRACT

A combination between a reductive and a holistic assay was employed to investigate whole fraction, synergistic, antagonistic and individual compound efficacy of vacuumdistilled turpentine fractions against the economically important brown-rot fungus *Coniophora puteana*. The fungus was subjected to recombinations of turpentine fractions at a concentration of 1000 ppm. All combinations exhibited useful antifungal properties, but some antifungal mixtures showed a more pronounced effect than the expected level of inhibition. Synergistic effects by a two-fold factor and minor antagonistic effects were observed. Complete growth inhibition of *C. puteana* was observed by a fraction obtained after distilling 1 L turpentine at 111–177 °C (0.5 mbar) as well as by mixing it with another fraction withdrawn at 70–79 °C (0.5 mbar). Chemical compositions of distilled fractions were determined through GC–MS analysis and Orthogonal Partial Least Squares (OPLS) multivariate data analysis of GC–MS chromatograms was employed to zoom in on the most active compounds responsible for antifungal activity. Isomers of epicubenol, the hydrocarbon aromatic compound ar-himachalene and α-cadinol are suggested as effective antifungal compounds. In addition, a subsequent fractionation of the most effective fraction was performed with preparatory gas chromatography and subfractions showed similar or better efficacy than previously observed. Our work demonstrates the possibility to retain adequate synergistic antifungal efficiency and offers an opportunity to explore the effects of individual compounds originating from the same crude sample.

1. Introduction

The readily available methods of combinatorial chemistry [1] and high throughput screening [[2], [3]] pushed phytochemicals from the spotlight and nowadays natural compounds is a frequently overlooked chemical space [4]. However, nature is a chemical factory that can produce compounds with high stereoselectivity, diversity and varying modes of action [5]. One main distinguishing feature of matrices from natural sources is their diversity in secondary metabolites [6–8]. As a result, researchers are met with a highly complex matrix, which challenges bioactivity assays [9]. With the arrival of more sophisticated analytical instruments and information extraction tools, scientists have yet again turned to nature as a potential discovery source of bioactives [10]. Even still, the evaluation, isolation and characterization of individual substances of such biologically active matrices are time-consuming and demanding. For identification of unknowns, an estimated price-tag of approximately $15 000 has been suggested [11] and oftentimes structural elucidation of known unknowns frequently occur [12]. Thus, there is a need for efficient methods that pinpoint vital areas where dereplication of matrix constituents and focused structure elucidation efforts need to occur.

Bioassay-guided fractionation followed by bioactivity assignment of complex matrices from natural sources commonly involve extensive utilization of partitioning and chromatographic techniques such as liquid-liquid extraction [13], solid-phase extraction [[14], [15]], liquid chromatography [16] and sparingly preparatory gas chromatography [17]. In contrast, usage of fractional distillation is limited due to the technique's inherent low resolution insofar as fractions end up with varying concentrations of its constituents. Separation of the natural matrix aims to reduce analytical complexity as well as boost chances of finding the bioactive component(s). However, natural extracts typically consist of more than one bioactive substance and loss of synergistic effects are frequently observed [18]. For proper bio(in)active assignment, it is therefore crucial that synergistic and antagonistic actions are

* Corresponding author.
E-mail addresses: joel.ljunggren@miun.se (J. Ljunggren), dan.bylund@miun.se (D. Bylund), bengt-gunnar.jonsson@miun.se (B.G. Jonsson), mattias.edman@miun.se (M. Edman), erik.hedenstrom@miun.se (E. Hedenström).

https://doi.org/10.1016/j.microc.2019.104325
Received 20 August 2019; Received in revised form 6 October 2019; Accepted 8 October 2019
Available online 19 October 2019

all considered or at least indicated when evaluating the effectiveness of fractionated natural extracts.

Deterioration in indoor and outdoor wood due to wood-decaying fungi incurs monumental economic losses each year [[19], [20]]. Heavy-metal as well as synthetic fungicide containing formulations are frequently used as impregnated or topically applied wood sentries to combat the fungal attack. The effectiveness of these compounds is unquestionable, however, many are leached to the environment where they cause harm to other species. Instead, applying biodegradable substances focused on excluding moisture in the wood, needed for fungal degradation, whilst simultaneously attacking fungal membranes is an interesting and eco-friendly solution. The identification and assessment of antifungal compounds from natural sources is therefore an active area of research [21].

The essential oil, turpentine, is produced as a by-product obtained in large quantities by steam distillation of Norway spruce (*Picea abies*) from the pulp and paper industry. Turpentine contains many of the compounds utilised by trees to protect against wood-decaying fungi and repel insect attack [22–24]. As a complex mixture of natural compounds, turpentine consists mainly of low molecular weight volatiles, i.e. terpenes, stilbenoids, aromatic and aliphatic compounds [[25], [26]]. Contrary to applying raw turpentine, extracting the most effective fractions is motivated in a biorefinery, and efficient use of a natural by-product, perspective. Oxygenated terpenoids, in particular, have shown to exhibit antimicrobial and synergistic, antagonistic and additive effects [27–29]. In a previous investigation by our group into the efficacy of steam distilled turpentine and subsequently fractionated turpentine, we observed both antagonistic and synergistic effect on the in vitro growth rate of the wood-decaying cellar-fungus *Coniophora puteana* (unpublished data).

As there are potentially monumental gains in finding synergism and likewise detrimental losses with antagonism, we aimed to devise a targeted approach towards finding the most plausible bioactive compound and its synergistic partners from vacuum distillation-fractionated turpentine. Herein, a laboratory study employing a D-optimal design and multivariate data analysis was conducted to assess compound interactions by mixing eco-friendly and biodegradable turpentine fractions and testing them against the wood-decaying fungi *C. puteana*. To our knowledge, this multivariate approach has not been scrutinized when screening for bioactive compounds from complex samples.

2. Materials and methods

2.1. Turpentine and fungal strain

Steam distilled turpentine was obtained from the thermo-mechanical pulp and paper mill SCA Ortviken (Sundsvall, Sweden). Turpentine (1 L) was previously divided into 23 fractions by vacuum distillation (see Table 1 for details). We previously assessed individual fractions of turpentine against this ubiquitous fungus on Hagem agar-plates (unpublished data). In accordance with the previous study, turpentine fractions 18–23 were selected for assessing growth inhibition of the wood-decaying fungus *Coniophora puteana* (KC491854.1). This fungus is one of the most damaging fungi in temperate and boreal forest areas and it is frequently associated with undesirable brown-rot, both indoors and outdoors [30].

Table 1
Distillation of turpentine fractions (Lindmark-Henriksson, 2003). The table has been truncated for brevity.

Fraction	Bp [°C] at P mbar	P [mbar]	Bp [°C] at 1010 mbar	Volume [ml]
1-17	20–53	18.6–0.8	135–240	787.5
18	61–74	0.5	297–315	26
19	70–79	0.5	308–320	18
20	79–87	0.5	320–335	33
21	89–95	0.5	340–347	23
22	100–111	0.5	350–370	10
23	111–117	0.5	370–380	10
Residue	>117	0.5	>380	92.5

2.2. Experimental design

Design of experiments (DOE) is a crucial planning step and an integral preceding part in chemometric analysis. The main goal of DOE is to retrieve as much information as possible in as few experimental runs as possible. For this purpose, several different designs have been devised, e.g. full factorial, fractional factorial, central composite (axial nodes are added) and D-optimal designs [[31], [32]]. Mixture designs present a unique constraint in that the sum of the ratios need to add up to one. This comes naturally as a concentration change in one constituent brings about a corresponding change in the other components. Not all designs can cope with such a constraint, but a D-optimal design can be used to set the sum of the ratios to 1. In addition, a D-optimal design has a lower number of runs, compared to full factorial designs when using six factors: a full factorial design has 64 runs while a D-optimal design has 28 runs. A quadratic D-optimal design was set up in MODDE 9.1 (Sartorius Stedim Data Analytics AB, Umeå, Sweden). A formulation factor between 0 and 0.75 including three technical replicates at a concentration of 1000 ppm (25 mg/plate) for a total of 32 samples was used. This concentration was selected on the basis that fractions should exhibit varying effects (unpublished data). Furthermore, each fraction on its own was added to the assay to establish baseline inhibition and to explore more of the model space, increasing the number of samples to 39. Samples were weighed and pooled gravimetrically and their ratios were recorded for *in silico* combination of GC–MS peak areas.

2.3. Bioassay and non-linear assessment

Turpentine fractions were added to the Hagem agar medium plates [33], stirred and poured into 9 cm Petri dishes. From a fresh culture inoculated one week before, a 3 mm agar plug of *C. puteana* was put face up onto the plates' centre in a sterile laminar flow cabinet. The inoculum plug was taken from actively growing hyphae at the perimeter of the fungus. After three days of inoculation, diametrical growth was measured in millimetres daily on the hour of inoculation for four days. *Coniophora puteana* grown on Hagem agar without supplement of turpentine was used as a positive control.

Non-linear effects have traditionally been expressed as fractional inhibitory concentration index (FICI), e.g. [34–36], where synergistic effects have been interpreted as (FICI $\leq$ 0.5); additive effects (0.5 < FICI $\leq$ 1); no interactive effect (1 < FICI $\leq$ 4) and antagonistic effects (FICI > 4). However, the magnitude of synergism using this approach is not readily apparent. Instead, we calculated the expected effect as $\Sigma r_f i_e$ where r_f is the ratio of the fraction in the mixture and i_e is each fractions individual effect at 1000 ppm. Consequently, fractions were assumed to exhibit a linear dose-response from 250 to 1000 ppm. Eq. (1) was used to estimate the magnitude of interaction (MOI) as a ratio centred around the observed growth rate for mixtures (m_e).

$$MOI = \frac{m_e - \sum r_f i_e}{m_e} \quad (1)$$

This approach allows a more straightforward interpretation as the magnitude will be represented by negative and positive values for synergistic and antagonistic effects, respectively.

2.4. Compound analyses

Analyses of turpentine constituents were performed by GC–MS as follows: 2 µl of fractions 18–23 were dissolved in 1 ml ethyl acetate

(Ethyl acetate HPLC grade, Fluka®) and 1 µl was injected with a GC sampler 80 (Agilent, Santa Clara, California, USA) into a 7890A GC (Agilent) split/splitless inlet coupled to an Agilent CP8944 column (30 m x 250 µm x 0.25 µm) using helium as carrier gas. Mass spectrometric detection was performed using a 240/4000 ion trap (Agilent) in full scan mode 50–500 *m/z* with 3 min solvent delay, 2 µScans averaged with a data rate of 1.12 Hz.

The following GC program was used: Inlet 275 °C, split 500, constant flow 1 ml/min of helium, temperature program 80 °C → 220 °C (2 °C/min) → 270 °C (10 °C/min), with a final hold of 10 min. The resulting mass chromatograms were analysed in Agilent MS Workstation 7.0.0 MS Data Review and peaks were manually integrated. Peak area retention times were corrected manually and absolute peak areas were used to construct the mixed fractions *in silico* using Microsoft® Excel 2016. Putative identification of eluted terpenes was performed using the NIST 17 and Wiley9 databases in MS Data Review. Additionally, Kováts retention indices were calculated using *n*-alkanes C8-C20 [37] and compared with those reported in the databases.

2.5. Multivariate analysis

To gain information from DOE, chemometrics methods are often used for data interpretation and there is, in principle, a plethora of different algorithms to use for the analysis of multivariate datasets. Perhaps two of the most commonly known techniques are Principal Component Analysis (PCA) and Partial Least Squares or Projection to Latent Structures (PLS) and its extensions orthogonal PLS (OPLS) and bidirectional PLS (O2PLS) [38–41]. Multivariate data analysis was performed in Simca-P 13.0.2 (Sartorius Stedim Data Analytics AB, Umeå, Sweden). Prior to analysis, variables were scaled to unit variance and OPLS models were set up with absolute peak areas of 128 peaks as x-variables and the average growth rate as y-variable. The predictability of the model was calculated by excluding observations spanning most of the space in the two first principal components. Remaining observations were fitted as a new model and the excluded observations were assigned as its prediction set. Root mean square error of prediction (RMSEP) for the new model was calculated according to Eq. (2).

$$RMSEP = \sqrt{\left(\frac{\sum (Y_{obs} - Y_{pred})^2}{N}\right)} \quad (2)$$

Two-sample weighted (w_i) pooled standard deviation (s_{pool}) for expected growth rates of mixtures were calculated according to Eq. (3)

$$s_{pool} = \sqrt{\frac{\sum_{i=1}^{N} w_i s_i^2}{n_1 + n_2 - 2}} \quad (3)$$

2.6. Preparatory GC

Based on the above results, the automated GC preparatory system, GC sampler 80 and a 7890A GC split (1:99) to a flame ionisation detector and a preparative fraction collector (PFC, Gerstel®) was used to further divide fraction 23 into subfractions 23.0–23.6. The following GC program was used with a CP8975 column (VF-5 ms, 30 m x 530 µm x 1 µm): 2 µl injection of fraction 23 with a concentration of 0.25 mg μl^{-1} (w/v). The split/splitless inlet was set to 275 °C, splitless, constant flow 9.5 ml/min of helium, initial oven temperature at 140 °C, hold 0.25 min → 240 °C (40 °C/min), 3 min hold and post-run 140 °C for 0.2 min. Total run time was 6 min x 100 runs; excluding cooldown. PFC parameters: transfer line 250 °C, switch temperature 260 °C and PFC-trap temperature was at room temperature with a fan as a cooling source. Seven traps from 0–6 were used for fraction collection where traps 0–2 were 100 µl traps and traps 3–6 were 1 µl traps.

Subfractions of fraction 23, denoted as 23.0 for the subfraction collected in trap 0, were collected at the following intervals: (23.0, 0–3.08 min and 5.5–6 min), (23.1, 3.08–3.48 min), (23.2, 3.48–3.52 min), (23.3, 3.52–3.60 min), (23.4, 3.60–4.27 min); (23.5, 4.27–4.42 min) and (23.6, 4.42–5.50 min). Trapped compounds were collected in conical vials by washing traps with ethyl acetate and flushing with argon.

2.7. External in vitro validation

Relative quantification of fraction 23 and its subfractions (23.0–23.6) with subsequent inoculation of C. *puteana* on the concentration corresponding to the previous 1000 ppm for each subfraction was performed. Subfractions of fraction 23 were analysed on the GC–MS system in triplicate measurement with the following GC program: Inlet 275 °C, split 500, constant flow 1 ml/min of helium, initial oven temperature 50 °C, 1 min → 220 °C (7 °C/min) → 270 °C (20 °C/min), 5 min. A split of 250:1 for trapped compounds with lower concentrations and split 500:1 for those with higher concentrations. The amount corresponding to a total concentration of 25 mg/plate of fraction 23 was calculated by taking the triplicate average area under the curve of three primary ions from three different peaks, if three peaks were present, for each trap and fraction 23. The ratio between fraction 23 and its subfractions was used to determine the volume of each fraction of 23. The calculated volumes were added to beakers and left in the hood to evaporate to dryness. Hagem agar was thereafter added to the beakers, autoclaved and poured into Petri dishes. Controls were: Fraction 23 as an interprotocol control prepared as previously described and *C. puteana* by itself as a positive control. No replicates were made due to the low amount of material obtainable through preparatory GC. Growth of *C. puteana* was recorded for six days after three days of inoculation.

3. Results and discussion

The economically important wood-decaying brown-rot fungus *C. puteana* was used to assess antagonistic and synergistic effects of turpentine fraction mixtures. A similar approach previously identified eugenol as an antimicrobial substance from a collection of one-hundred and fifty-eight essential oils [42]. Whereas they used different natural sources, we performed comparable work using the same raw material. By mixing fractions according to a quadratic D-optimal design, the parametrical search space increases and enables a deeper probing into the causation of the underlying bioactive effects of turpentine fractions.

3.1. Composition and effectiveness of turpentine fractions against C. puteana

Fractionation of turpentine revealed 128 compounds, with 76 putatively identified compounds containing some that would otherwise be undetectable in a crude sample injection. Fractions were generally complex and individual fractions consisted of approximately 91 compounds in varying concentrations (Table 2). The main constituents of crude turpentine are 74% monoterpenes, 13% sesquiterpenes, 1% diterpenes and 12% high molecular weight compounds such as the resinous acids (palmitic, pimaric, abietic, dehydroabietic, behenic, isopimaric) [26]. In comparison, 1,10-diepicubenol, the compound present in the highest concentration in fraction 23 accounts for only 0.15% in crude turpentine. The lowest boiling fraction consisted mostly of the sesquiterpenes α-gurjunene, longifolene and α-terpineol while fraction 23 was abundant in the sesquiterpene δ-cadinene, the oxygenated sesquiterpene 1,10-diepicubenol and the diterpene cembrene. It is commonly assumed that the bioactivity of essential oils is principally caused by their major components [43–46]. In contrast, other research has demonstrated that minor components of essential oils are critical to synergistic activity [47].

In this work, we exclusively assayed those minor components. All fractions of turpentine as well as turpentine fraction mixtures were

Table 2

Turpentine constituents and their relative composition in each fraction. RM and FM refer to reverse (R) and forward (F) library matches while RKI and MKI denote reference and measured Kovát's index, respectively. The type column symbolises the compound class as: A = Aromatic; AH = Aldehydic terpene; D = Diterpene; S = Sesquiterpene; HS = Hydroxylated sesquiterpene; HT = Hydroxylated monoterpene; and UA = unsaturated aldehyde. The relative composition of fraction 18–23 is shown on the right-hand side. Missing values indicate absence or a relative composition below 1%.

RT [min]	Compound	CAS	RM	FM	MW	RKI	MKI	Type	18	19	20	21	22	23
9.01	Fenchol	1632-73-1	874	874	154	1113	1109	HT						
9.90	Sabinol		865	859	152	1143	1132	HT						
10.68	Phenol, x-Ethyl	90-00-6	979	942	122	1169	1152	A						
11.10	p-mentha-1,5-dien-8-ol	1686-20-0	791	658	152	1167	1163	HT						
11.20	Unknown						1165		1%					
11.53	Terpinen-4-ol	562-74-3	834	821	154	1177	1174	HT						
11.77	Benzenemethanol	1197-01-9	825	825	150	1183	1180	A						
11.85	Unknown				154	1189	1182	HT						
12.16	α-terpineol	10482-56-1	893	893	154	1190	1190	HT	9%	1%				
12.27	Myrtenol	515-00-4	834	820	152	1195	1193	HT						
12.5	Unknown	128-50-7	769	769	166	1202	1199	HT						
12.79	Verbenone	1196-01-6	867	867	150	1204	1205	KT						
13.26	Trans-carveol	1197-07-5	845	845	152	1217	1214	HT						
13.72	Thymol methyl ether	31574-44-4	903	895	164	1230	1224	A						
13.9	Cis-carveol	1197-06-4	786	754	152	1229	1227	HT						
14.06	3,4-Dimethoxytoluene	494-99-5	876	847	152	1233	1231	A						
14.49	Unresolved						1240							
14.75	Unresolved						1245							
15.02	P-carvomentheone	89-81-6	840	835	152	1253	1250	KT						
15.36	Unknown						1257							
15.51	Unknown						1261							
15.97	p-ethylguaiacol	2785-89-9	913	837	152	1282	1270	A						
16.25	Phellandral	21391-98-0	799	744	152	1276	1276	AH						
16.53	(-)-Bornyl acetate	5655-61-8	906	906	196	1284	1281	Ester	2%					
16.71	α-terpinen-7-al	1197-15-5	751	697	150	1283	1285	AH						
16.89	Cuminol	536-60-7	872	858	150	1289	1289	A						
17.10	Unresolved						1293							
17.26	Unresolved	89-83-8	894	819	150	1290	1296							
17.82	Car-3-en-5-one	81800-50-2	817	772	150	1314	1307	AH						
17.97	Unknown						1310	HT						
18.35	2,4-decadienal	25152-84-5	861	861	152	1317	1317	UA	1%					
18.69	Unknown						1323	S						
19.13	Bicyclo[4.3.0]nonane, 7-methylene-2,4,4-trimethyl-2-vinyl		837	827	204		1331	S		1%				
19.85	α-copaene	3856-25-5	852	828	204		1344	S	4%	2%				
20.01	α-longipinene	5989-08-02	880	880	204	1353	1347	S	7%	4%	1%			
20.88	Unknown						1363							
20.99	Unknown						1365							
21.07	Ylangene	14912-44-8	904	889	204	1372	1366	S	7%	6%	1%			
21.34	Longicyclene	1137-12-8	903	903	204	1374	1371	S	1%	1%				
21.42	Copaene	3856-25-5	901	896	204	1376	1373	S	2%	2%	1%			
21.64	Unknown						1377							
21.91	2-epi-α-Funebrene α-Cedrene α-Cedrane	65354-33-8 469-61-4 13567-54-9	867 858 843	863 848 837	204 204 206		1382	S						
22.09	epi-Sesquithujene	159407-35-9	828	828	204	1391	1385	S						
22.20	β-Elemene	515-13-9	870	840	204	1391	1387	S						
22.32	Sativen	3650-28-0	858	858	204	1396	1389	S	1%	1%				
22.81	(Z)-β-Caryophyllene				204	1406	1398	S						
22.94	α-Gurjunene	489-40-7	875	875	204	1411	1401	S	25%	29%	12%	1%		
23.29	Longifolene	475-20-7	913	913	204	1413	1407	S	14%	18%	7%			
23.65	Di-epi-α-cedrene	50894-66-1	858	837	204	1427	1413	S	1%	2%	1%			
23.85	trans-Caryophyllene	87-44-5	898	898	204	1423	1417	S	2%	1%	1%			
24,00	Unknown						1419	S						
24.13	Unknown sesquiterpene				204		1422	S						

(*continued on next page*)

Table 2 (*continued*)

24.23	Unknown sesquiterpene				204		1423	S									
24.43	Unknown sesquiterpene				204		1427	S									
24.63	Unknown sesquiterpene				204		1431	S	1%	2%	2%						
24.74	Unknown sesquiterpene				204		1433	S									
25.01	Unknown sesquiterpene				204		1437	S									
25.37	Benzene, 1-(1,5-dimethylhexyl)-4-methyl-	1461-02-5	774	745	204	1448	1444	A									
25.54	α-Himachalene	3853-83-6	867	864	204	1449	1447	S	1%		1%	1%					
25.79	α-Humulene	6753-98-6	806	806	204	1454	1451	S			1%						
26.10	Unknown				204		1457	S									
26.51	Unresolved Acoradiene	24048-44-0	845	810	204	1471	1464	S									
26.99	γ-Muurolene	30021-74-0	896	896	204	1477	1472	S	1%	4%	6%	5%	1%	1%			
27.17	γ-Himachalene	53111-25-4	831	831	204	1488	1476	S			1%	1%	1%				
27.30/ 27.35	Unresolved Germacrene D/ α-Curcumene	23986-74-5/ 644-30-4	905/ 895	905/ 838	204	1482/ 1488	1477	S/A	5%	4%	10%	5%	2%				
27.52	Aristolochene	26620-71-3	751	695	204	1494	1482	S									
27.74	β-Selinene	17066-67-0	896	827	204	1493	1486	S			1%						
27.98	Unknown sesquiterpene				204		1490	S		1%	2%	2%	1%	1%			
28.16	Valencen	4630-07-03	805	764	204	1503	1493	S			1%	1%					
28.35	Unknown sesquiterpene				204		1496	S	1%	2%	5%	7%	5%	3%			
28.54	δ-Guaiene	3691-11-0	832	830	204	1505	1500	S			1%	1%					
28.86	Unresolved						1506					1%	2%	1%			
29.01	α-Dehydro-ar-himachalene	78204-62-3	931	874	200	1516	1508	A				4%	2%	1%			
29.13	α-Amorphene	23515-88-0	854	847	204	1538	1510	S	1%	2%	5%	8%	7%	3%			
29.44	δ-Cadinene	483-76-1	884	884	204	1524	1516	S	3%	2%	24%	37%	34%	15%			
29.61	Calamenene	483-77-2	870	853	202	1523	1519	S	1%	2%	3%	4%	5%	2%			
29.92	Unknown						1525	A									
30.21	ar-Himachalene	19419-67-1	873	851	202	1542	1530	A			1%	2%	3%	5%			
30.44	α-cadinene	11044-40-9	883	849	204		1534	S			1%	2%	2%	2%			
30.69	calacorene		959	917	172	1542	1538	A			1%	3%	5%	3%			
30.88	Unresolved						1542										
31.24	Unresolved						1548					1%					
31.47	Unknown						1552					1%	1%	1%			
31.85	β-Calacorene	50277-34-4	929	926	200	1563	1559	A									
31.93	Similar to β-Calacorene	50277-34-4	890	850	200	1563	1560	A									
32.12	1,5-Epoxysalvial-4(14)-ene	88395-47-5	795	769		1573	1564	Eter					1%	1%			
32.27	Spathulenol	6750-60-3	738	737	220	1576	1567	HS									
32.39	Unknown						1569										
32.55	Unresolved						1571										
32.64	Unknown						1573										
32.88	Caryophyllene oxide	1139-30-6	855	855	220	1581	1577	Epoxide		1%							
33.12	Axenol	72203-99-7	867	861	222	1586	1582	HS						1%			
33.27	Unknown						1584				1%	2%	4%	6%			
33.50	Salvial-4(14)-en-1-one					1595	1588	HS					1%	1%			
33.62	Unknown						1591										
33.79	Unknown						1594										
33.99	Longiborneol	465-24-7	836	831	222	1607	1597	HS					1%	1%			
34.33	Unresolved						1603							1%			
34.42	Humulene epoxide II	19888-34-7	814	802	220	1606	1605	HS									
34.60	Unknown						1608										
34.88	Epicubenol	19912-67-5	785	781	222	1627	1614	HS				1%	2%	4%			
35.45	1,10-Diepicubenol	73365-77-2	863	852	222	1636	1624	HS			1%	3%	8%	15%			
35.79	Unknown						1630										
36.05	Unknown						1635										
36.25	α-cadinol	481-34-5	851	784	222	1653	1639	HS				1%		4%			
36.36	epi-α-muurolol	19912-62-0	820	786	222	1660	1641	HS					1%	2%			
36.51	Torreyol	19435-97-3	788	759	222	1653	1644	HS					1%	2%			

(*continued on next page*)

Table 2 (*continued*)

36.82	epi-α-Cadinol	5937-11-1	882	828	222	1649	1649	HS					
36.96	Unknown						1652					2%	5%
37.12	Unknown				220		1655	HS					1%
37.48	10-Hydroxycalamene	123931-36-2	862	862	218	1666	1661	A	1%				
37.57	Unknown						1663						
37.88	Cadalene	483-78-3	944	935	198	1688	1669	A				1%	2%
38.03	Unknown						1672						
38.60	Unknown	81968-62-9	825	822	220	1695	1682	A					1%
38.82	7-Isopropyl-4,10-dimethylenecyclodec-5-enol	81968-62-9	825	822	220	1695	1686	A				1%	2%
39.19	Unknown						1693						
39.41	4-Isopropyl-6-methyl-1-tetralone	57494-10-7	796	796	202	1716	1697	A					
39.68	Unknown						1702						1%
40.59	Unknown						1719						
43.74	Isovalencenol	22387-74-2	793	776	220	1788	1780	HS					
46.28	Unknown						1830						
47.43	Unknown						1852						
50.45	Cembrene	1898-13-1	890	890	272	1939	1913	D				2%	8%
51.92	Cembrene A	31570-39-5	872	841	272	1959	1944	D					
52.30	geranyl-α-terpinene					1962	1952	D					
53.73	Unknown						1982						
54.70	Unknown						2002*						

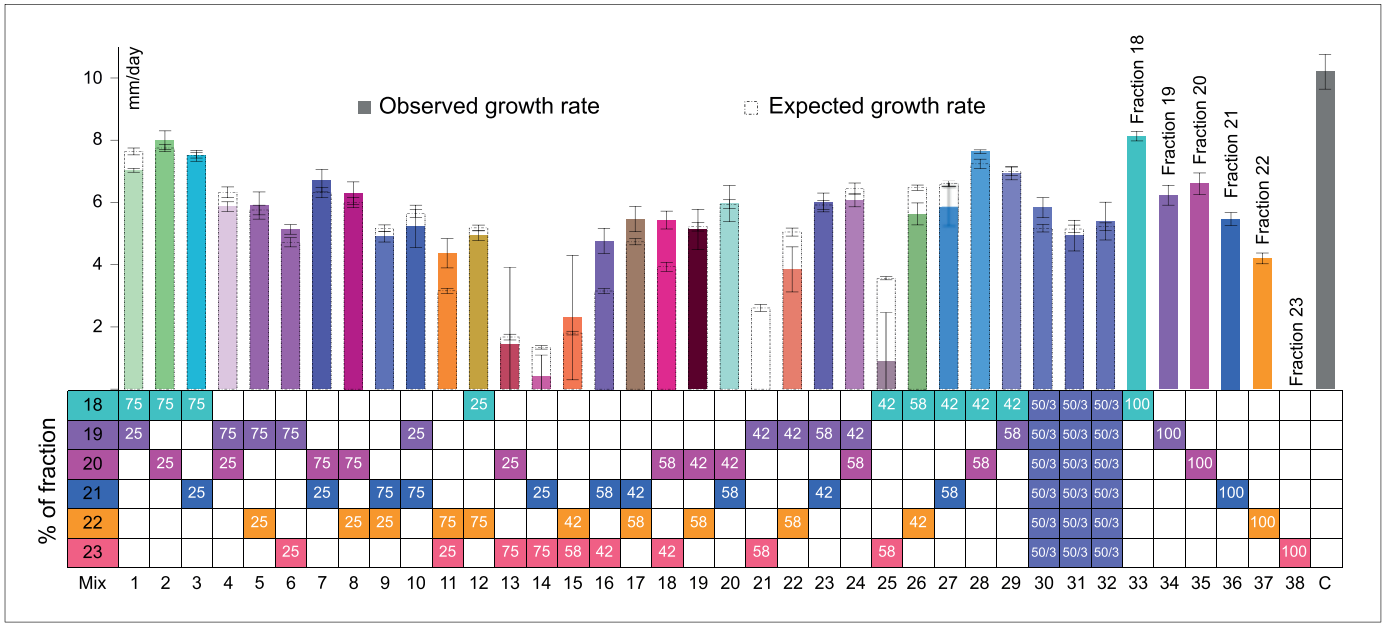

Fig. 1. Growth rate of C. puteana on Hagem agar supplemented with different proportions of fractionated turpentine. Coloured bars, according to the color mix of pure fractions, show the observed growth rate while dashed bars show expected growth rate when mixing pure fractions. The percentage of each fraction added to mixtures is shown below each bar. Error bars denote 95% confidence intervals. Expected growth rate confidence intervals are based on the pooled and weighted standard deviation at the same significance level of $p < 0.05$.(For interpretation of the references to color in this figure legend, the reader is referred to the web version of this article.)

significantly different from the control according to Student's *t*-test (p-values all below 0.005). For the individual fractions, hydrocarbon sesquiterpenes demonstrated lower antifungal efficacy while an increasing inhibition towards the oxygenated sesquiterpenes can be seen in Fig. 1. It is known that fungi produce hydrocarbon sesquiterpenes and they should be naturally habituated towards them, but only a few fungal oxygenated sesquiterpenes have been reported [48]. For instance, growth of *C. puteana* was entirely inhibited by heartwood essential oil of *Cupressus atlantica* at 900 ppm with an approximate composition of 2.4% hydrocarbon monoterpenes, 44% oxygenated monoterpenes, 13% hydrocarbon sesquiterpenes and 33% oxygenated sesquiterpenes [49]. Moreover, an induced systemic response comparable to fungal attack can be mediated by the application of methyl jasmonate. Following the systematic onset of Norway spruce defensive mechanisms by the substance, significantly increased levels of monoterpenes after 10–15 days is followed by raised diterpene levels after approximately 10 days. However, sesquiterpene concentrations remain relatively unaltered [50]. Congruent with the steady-state of hydrocarbon sesquiterpenes after defence induction, fractions 18–22 that chiefly contain these sesquiterpenes exhibited the lowest overall activity against *C. puteana* (Table 2). Hence, our study supports the fact that oxygenated terpenes are more effective as antifungal agents than

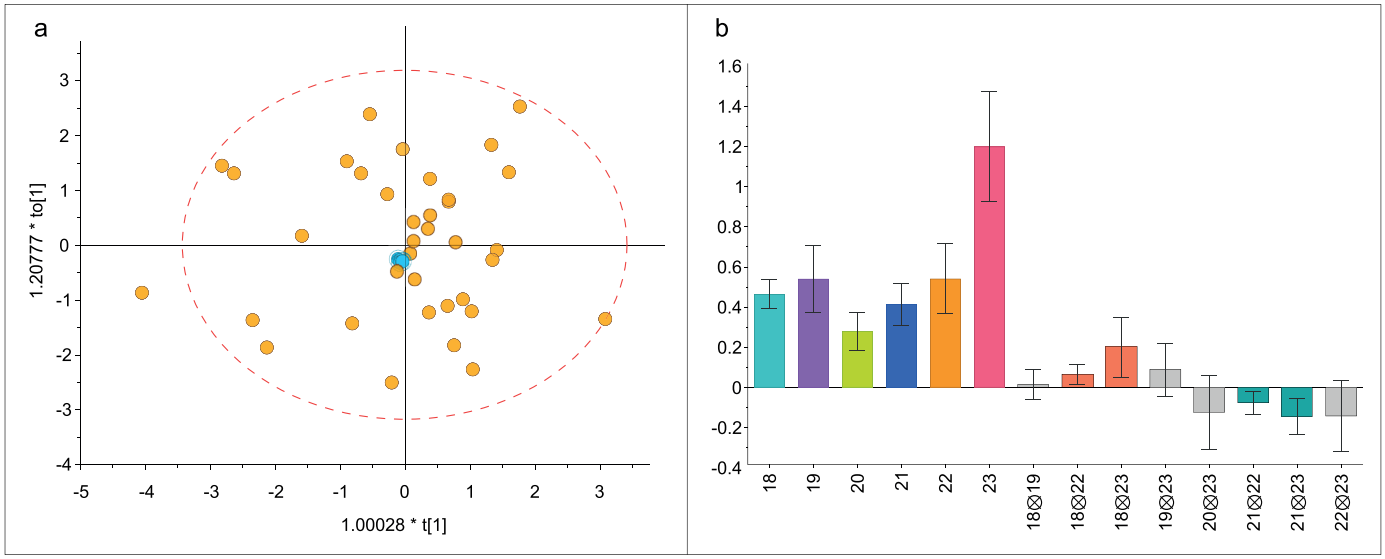

Fig. 2. OPLS regression model, with cross-terms purviewed from Fig. 1, [OPLS, $R^2X_{(cum)} = 0.768$; $R^2Y_{(cum)} = 0.892$; $Q^2_{(cum)} = 0.851$, (1 + 7)]. a) Depict the score-plot of the model with center replicates highlighted in cyan color. b) Show the coefficients of normalized growth rate reduction where 1 = complete inhibition. Cross-terms indicate the estimated non-linear effects.(For interpretation of the references to color in this figure legend, the reader is referred to the web version of this article)

their hydrocarbon counterparts. A sharp increase in growth inhibition potential of turpentine fraction on *C. puteana* can be seen from fractions 22–23 (Fig. 1). Fraction 23 is the only fraction containing diterpenes and the marked activity may have been attributable to their presence, as seen by the production of this compound class following defence induction [50].

In relation to the other fractions, the sudden and complete growth inhibition property of fraction 23 against *C. puteana* was striking (Fig. 1). Nevertheless, the actual growth rate efficacy of fraction 23, as measured in mm day^{-1}, was left undetermined. This would implicate calculations and non-linear effects could falsely be determined as relevant. By solving the overdetermined system of linear equations in Fig. 1, the effect of fraction 23 at 1000 ppm was estimated as -0.513 mm day^{-1} with a relatively large residual of 0.33 mm day^{-1}. This estimation was subsequently used in all non-linear effect calculations.

3.2. Non-linear effects

One objective of this study was to investigate if non-linear effects could be identified when recombining fractions. Growth rate of the brown-rot fungi *C. puteana* growing on agar plates supplemented with mixed and individual turpentine fractions are shown in Fig. 1. The mixtures showed the presence of expected linear effects but also synergistic and minor antagonistic effects. In general, most combinations showed linear behaviour with the MOIs centred close to zero. On the other hand, strong synergistic growth-inhibiting effects were most noticeable for M21 as the MOI was immeasurable due to the observed growth rate of 0 mm day^{-1}. Other synergistic effects were noticed for M25 and M14 with MOIs of -2.6 and -1.4, respectively. In contrast, the highest antagonistic MOI was observed for M16 with MOI = 0.38. Other potentially antagonistic interactions were observed for mixtures M6, M11, M18 and M28. In our case, the observed non-linear effects are not caused by additive synergism, as the mixing of fractions is a zero-sum approach.

Despite rigorous methods for adding turpentine and inoculum plug, a high variation was observed for M13 and M25 where only one replicate grew. For mixture 15, only two replicates grew. This should signify that the applied substances were close to the biocidal threshold and that the fungus could overcome its hostile environment due to tiny variances in experimental conditions.

An additional test for non-linear effects using a chemometrics approach was employed. Multivariate data analysis of fractions with unit variance scaled OPLS-models with no interaction terms [OPLS, $R^2X_{(cum)} = 0.403$; $R^2Y_{(cum)} = 0.833$; $Q^2_{(cum)} = 0.81$, (1 + 2) components] was contrasted with all cross interaction terms [OPLS, $R^2X_{(cum)} = 0.43$; $R^2Y_{(cum)} = 0.873$; $Q^2_{(cum)} = 0.821$, (1 + 5)] and cross interaction terms from potentially synergistic and antagonistic mixtures as observed in Fig. 1 [OPLS, $R^2X_{(cum)} = 0.768$; $R^2Y_{(cum)} = 0.892$; $Q^2_{(cum)} = 0.851$, (1 + 7)]. The latter model showed the highest predictive power and its score plot is shown in Fig. 2a. The scores show that the nine center replicates are clustering close to the origin. The combination of the score-wise dispersion pattern, the center-clustering of technical replicates and their principally accurate estimation of their antifungal effect from individual fractions (Mix 30–32, Fig. 1) suggest a linear dose-response for individual fractions at the tested concentration range. Coefficients of interaction terms 18⊗22 and 18⊗23 were indicated as having synergistic effects on fungal growth (Fig. 2b). The cause of synergism may stem from: differential action on the same or different targets in regulatory pathways; inhibition of necessary biodegradation enzymes to improve bioavailability of the active compound (s); or overcome resistance mechanisms [27]. According to the same model, interactions 21⊗22 and 21⊗23 have an antagonistic effect on *C. puteana* fungal growth rate when mixed together. Mechanism of interactions that produce antagonistic effects have been less studied and usually originate from same-target competition or chemical interaction among compounds [47].

Non-linear effects on a per compound basis revealed an antagonistic effect between the sesquiterpene δ-cadinene and the hydroxylated sesquiterpene 1,10-diepicubenol by a cross-interaction model [OPLS, $R^2X_{(cum)} = 0.903$; $R^2Y_{(cum)} = 0.857$; $Q^2_{(cum)} = 0.8$, (1 + 6) components]. The results are presented in-text due to clarity difficulties when making interaction plots with a large number of variables. Sesquiterpenes cadinene, muurolene, calamene and α-amorphene also showed potential antagonism with the oxygenated sesquiterpenes and the diterpene cembrene. Due to the high efficacy of fraction 23 in comparison with the other individual fractions, the lower efficacy of mixtures may also occur by dilution of the more potent substances present in the fraction. The hydroxylated sesquiterpene α-cadinol seems to be involved in both synergistic and antagonistic activity with 1,10-diepicubenol and δ-cadinene, respectively.

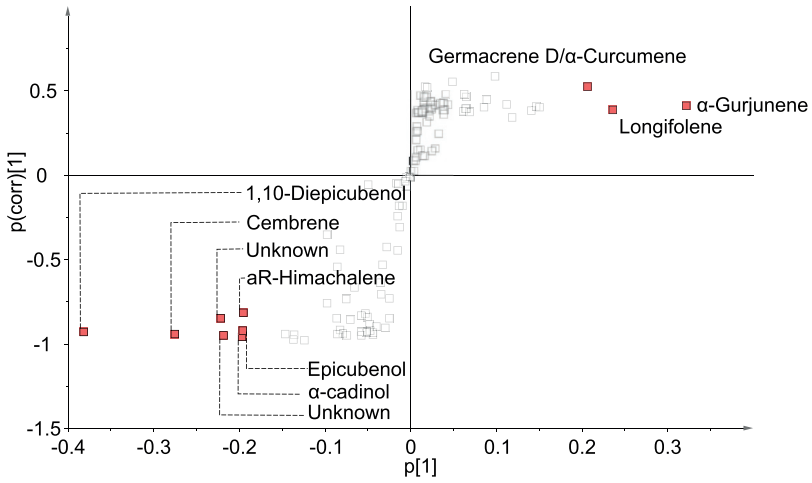

Fig. 3. S-plot of regression model [OPLS, $R^2X_{(cum)} = 0.954$; $R^2Y_{(cum)} = 0.83$; $Q^2_{(cum)} = 0.817$, (1 + 3)] with individual constituents of recombined turpentine fractions against *C. puteana* growth rate. Compound position along the p[1]-axis denote variable magnitude while the p(corr)[1]-axis show each compounds correlation. Empty boxes show positions of the remaining unnamed compounds.

3.3. Estimation of individual compound efficacy

As discussed above, the topic of non-linear effects was one goal with this study but we also aimed to assess the efficacy of each individual compound. For this purpose, an OPLS model of the D-optimal mixture design with one predictive and three orthogonal principal components was setup [$R^2X_{cum} = 0.954$, $R^2Y_{cum} = 0.83$, $Q^2_{cum} = 0.817$]. Statistical validity of the model was examined by fitting a new model to 100 random permutations of the response variable and comparing R^2_{cum} and Q^2_{cum} with the original model. The line going through the new models intersected the y-axis at -0.22 and 0.01 for Q^2_{cum} and R^2_{cum}, respectively. If the permuted models consistently display lower values for both parameters, the original model is unlikely to have arisen out of pure chance. We thus estimated that the model correlated well with the fungal growth rate. Sixteen random samples spanning the observational space were used as prediction set and a new OPLS model ($R^2X_{cum} = 0.954$, $R^2Y_{cum} = 0.839$, $Q^2_{cum} = 0.819$) was built with the remaining observations. Predicted scores of the prediction set (data not shown) closely overlapped with their respective positions in the original model and RMSEP was found to be 1.2 mm day^{-1} for this internal test set. Combined, these results indicate a statistically robust model. It should, however, be kept in mind that the first and last distilled fractions are underrepresented in the model, given that the concentration of their individual constituents cannot be altered to the same extent as fractions in the middle.

Interesting turpentine components connected to *C. puteana* growth are shown in Fig. 3. The two diastereomers epicubenol and 1,10-diepicubenol were found as potentially efficient antifungal compounds. Literature regarding the diastereomers antifungal activity on wood-decaying fungi only include them as minor components in essential oils from other sources and is similarly of minor value for approximating their efficacy. Herein, we provide the first wood-decaying antifungal activity using these diastereomers as major components. The cadinane sesquiterpenoid α-cadinol was likewise indicated as a potential antifungal. It has previously been shown to completely inhibit other basidiomycota members, namely, *Trametes versicolor* and *Laetiporus sulphureus* at a concentration of 100 ppm [51]. Structure-activity relationship investigation revealed that a double bond in a trans configuration coupled with an equatorial hydroxyl group showed the highest activity. The stereochemistry at the hydroxyl group was less crucial for activity than the geometric configuration of the double bond in the ring. Additionally, a correlation with the hydrophobicity of cadinol derivates revealed that more hydrophobic derivates were more effective [52]. Given that the double bond geometry is the same for both substances, the activity of α-cadinol (XLogP3-AA = 3.3) could be slightly higher than the structurally related isomers of cubenol

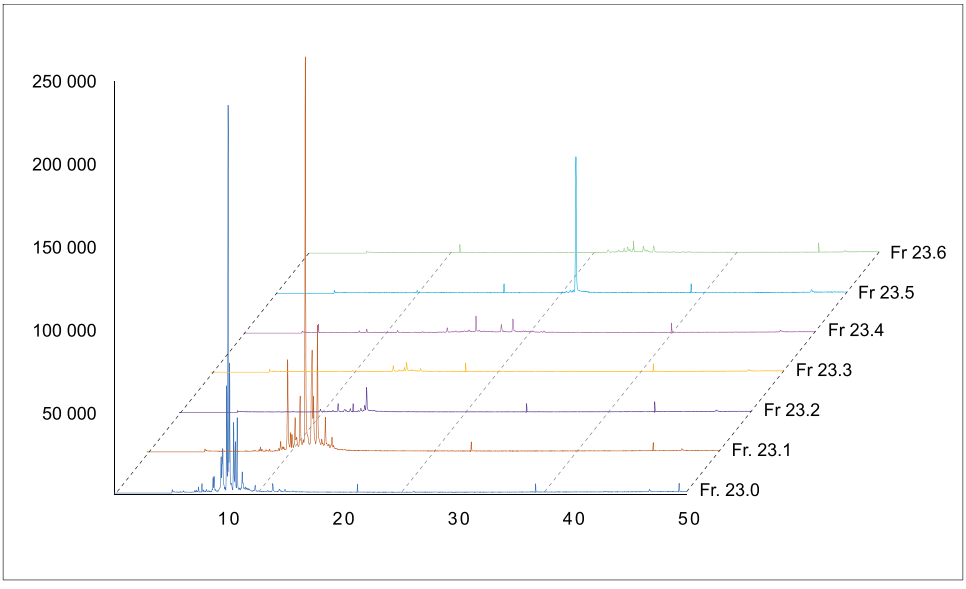

Fig. 4. Mass chromatograms after preparatory GC of turpentine fraction 23. The x-axis show retention time and y-axis mass counts.

(XLogP3-AA = 3.7) and its epimers.

Contrary to the inhibition indicated for the α-cadinol and cubenol epimers, the sesquiterpenes α-gurjunene, longifolene and possibly germacrene show an opposite or lower effect (Fig. 3). This is curious since the latter compounds are present in high amounts in both fraction 18 and fraction 19 that showed low individual activity but high synergistic activity. A reasonable explanation could be a differential mode of action or that minor components in those lower-boiling fractions exhibit stronger than expected synergistic effects.

Such low-level compounds that also demonstrate a different mechanism may be aromatic compounds. Especially aromatics with a hydroxyl group such as carvacrol and thymol, are highly effective antifungal agents down to 79.8 ppm against *Saccharomyces cerevisiae* [53]. Interestingly, hydrophobicity alone cannot explain the observed efficacy as *p*-cymene, a precursor of carvacrol with a higher lipid partition coefficient, is non-toxic. The hydroxyl group of carvacrol is crucial for toxicity in single-cell microorganisms as noticed against *Bacillus cereus* [54] and enzyme inactivation has been presented as the fundamental mechanism for the toxicity of phenolic compounds [55]. The S-plot shown in Fig. 3 indicates ar-himachalene as the most effective aromatic in turpentine fractions. Ar-himachalene, contrarily, lacks this crucial moiety and the modelled effect is therefore questionable. This shows that individual estimation of a compound's efficacy is non-trivial and that further studies with isolated ar-himachalene are necessary to thoroughly establish this compound and the other compounds as effective antifungal agents.

3.4. Efficacy of fraction 23 subfractions

To verify or reject assumptions based on the model, preparatory GC was used to further divide fraction 23 into subfractions (23.0 - 23.6, Fig. 4). The cut-off, corresponding to 0–31.6 min, was selected so that subfraction 23.0 was constituted mainly of the sesquiterpenes α-amorphene and δ-cadinene as well as ar-himachalene. It was thus separated from the hydroxylated sesquiterpenes epicubenol and 1,10-diepicubenol in subfraction 23.1 (31.6–38.2 min). Furthermore, the cut-off of subfraction 23.5 was selected to enrich the diterpene cembrene. The trend ($n = 1$) in growth rates for subfractions were, in ascending order: Fr23 = 23.0 = 23.1 (0 mm/day), 23.5 (6.6 mm/day), 23.3 (6.94 mm/day), 23.4 (7.2 mm/day), 23.6 (7.2 mm/day), control (8.1 mm/day), 23.2 (8.3 mm/day). Subfractions 23.0 and 23.1 completely inhibited growth of *C. puteana* at their approximately corresponding concentration levels when undivided fraction 23 was applied.

According to the cross-term OPLS model with individual compounds, subfraction 23.0 constituents are less effective than subfraction 23.1 that contains most of the potent inhibitory compounds. This result was uncorroborated after preparatory GC, which suggests that ar-himachalene may still be a potent antifungal compound even without the hydroxyl moiety, as mentioned in the final paragraph of Section 3.3.

In Section 3.1, the presence of diterpenes was suggested as a possible reason for the increased inhibitory effect of fraction 23 (Fig. 1). Our model also supported this claim (Fig. 3). Yet, the isolation of the diterpene cembrene did not exhibit a strong antifungal effect. The weak activity contra the predicted effect of cembrene is potentially caused by the loss of synergism or due to its correlation with other constituents of fractions 23, thereby boosting its relevance in the model. The ambiguous interpretation of cembrene underlines the need for further testing, as well as more efficient strategies for the decorrelation of matrix constituents.

4. Conclusions

We explored the recombination of a fractionated mixture to estimate non-linear and antifungal efficacy of individual compounds. Both synergistic and antagonistic effects were detected by mixing turpentine fractions. For compound assessment, we performed preparatory GC that corroborated ar-himachalene as a putative antifungal compound. This separation also allowed us to strengthen our suggestion of the oxygenated sesquiterpene 1,10-diepicubenol as a potent *C. puteana* growth inhibitor. Taken together, our study highlights the possibility to recover synergistic effects by recombining turpentine fractions for efficient antifungal use of turpentine.

Declaration of Competing Interest

The authors declare that they have no known competing financial interests or personal relationships that could have appeared to influence the work reported in this paper.

Acknowledgements

This project was made possible with the funding from the EU Structural Fund (ID00156708/Mål 2) and the County Administrative Board of Västernorrland (ID193119). The authors are thankful to Oddmund Björkås at SCA Ortviken, Sweden, for providing turpentine and to Mikael Gudrunsson for laboratory assistance.

Supplementary materials

Supplementary material associated with this article can be found, in the online version, at doi:10.1016/j.microc.2019.104325.

References

[1] D. Brown, Future pathways for combinatorial chemistry, Mol. Divers. 2 (1997) 217–222.
[2] J.J. Agresti, E. Antipov, A.R. Abate, K. Ahn, A.C. Rowat, J.-C. Baret, M. Marquez, A.M. Klibanov, A.D. Griffiths, D.A. Weitz, Ultrahigh-throughput screening in drop-based microfluidics for directed evolution, Proc. Natl. Acad. Sci. 107 (2010) 4004–4009.
[3] C. McInnes, Virtual screening strategies in drug discovery, Curr. Opin. Chem. Biol. 11 (2007) 494–502.
[4] A.L. Harvey, R. Edrada-Ebel, R.J. Quinn, The re-emergence of natural products for drug discovery in the genomics era, Nat. Rev. Drug Discov. 14 (2015) 111–129.
[5] R.K. Allemann, Chemical wizardry? The generation of diversity in terpenoid biosynthesis, Pure Appl. Chem. 80 (2008) 1791–1798.
[6] I. Castellanos, F.J. Espinosa-García, Plant secondary metabolite diversity as a resistance trait against insects: a test with *Sitophilus granarius* (Coleoptera: Curculionidae) and seed secondary metabolites, Biochem. Syst. Ecol. 25 (1997) 591–602.
[7] H. Jenke-Kodama, R. Müller, E. Dittmann, Evolutionary mechanisms underlying secondary metabolite diversity, Prog. Drug Res. (2008) 120–140.
[8] M.P. Speed, A. Fenton, M.G. Jones, G.D. Ruxton, M.A. Brockhurst, Coevolution can explain defensive secondary metabolite diversity in plants, New Phytol. 208 (2015) 1251–1263.
[9] J.L. Wolfender, M. Litaudon, D. Touboul, E.F. Queiroz, Innovative omics-based approaches for prioritisation and targeted isolation of natural products-new strategies for drug discovery, Nat. Prod. Rep. 36 (2019) 855–868.
[10] J.L. Wolfender, G. Marti, A. Thomas, S. Bertrand, Current approaches and challenges for the metabolite profiling of complex natural extracts, J. Chromatogr. A 1382 (2015) 136–164.
[11] A. Bouslimani, L.M. Sanchez, N. Garg, P.C. Dorrestein, Mass spectrometry of natural products: current, emerging and future technologies, Nat. Prod. Rep. 31 (2014) 718–729.
[12] J. Hubert, J.-M. Nuzillard, J.-H. Renault, Dereplication strategies in natural product research: how many tools and methodologies behind the same concept? Phytochem. Rev. 16 (2017) 55–95.
[13] A. Fagerlund-Edfeldt, E. Hedenström, M. Edman, B.G. Jonsson, Effect of debarking water from norway spruce (*Picea abies*) on the growth of five species of wood-decaying fungi, Z. Naturforsch. C - A J. Biosci. 9–10 (2014) 418–424.
[14] A. Cutignano, G. Nuzzo, A. Ianora, E. Luongo, G. Romano, C. Gallo, C. Sansone, S. Aprea, F. Mancini, U. D'Oro, A. Fontana, Development and application of a novel SPE-method for bioassay-guided fractionation of marine extracts, Mar. Drugs 13 (2015) 5736–5749.
[15] L.T. Khoo, J.O. Abdullah, F. Abas, E.R.M. Tohit, M. Hamid, Bioassay-guided fractionation of *Melastoma malabathricum* Linn. leaf solid phase extraction fraction and its anticoagulant activity, Molecules 20 (2015) 3697–3715.
[16] E. Hedenström, A. Fagerlund Edfeldt, M. Edman, B.-G. Jonsson, Resveratrol, piceatannol, and isorhapontigenin from Norway spruce (*Picea abies*) debarking wastewater as inhibitors on the growth of nine species of wood-decaying fungi, Wood Sci. Technol. 50 (2016) 617–629.
[17] R. Rahmani, F. Andersson, M.N. Andersson, J.K. Yuvaraj, O. Anderbrant, E. Hedenström, Identification of sesquisabinene B in carrot (*Daucus carota* L.) leaves

as a compound electrophysiologically active to the carrot psyllid (*Trioza apicalis* Förster), Chemoecology 29 (2019) 103–110.
[18] T. Inui, Y. Wang, S.M. Pro, S.G. Franzblau, G.F. Pauli, Unbiased evaluation of bioactive secondary metabolites in complex matrices, Fitoterapia 83 (2012) 1218–1225.
[19] A.D. Rayner, L. Boddy, Fungal Decomposition of wood. Its biology and Ecology, John Wiley & Sons Ltd., 1988.
[20] F.O. Asiegbu, A. Adomas, J. Stenlid, Conifer root and butt rot caused by *Heterobasidion annosum* (Fr.) Bref. s.l, Mol. Plant Pathol. 6 (2005) 395–409.
[21] T. Singh, A.P. Singh, A review on natural products as wood protectant, Wood Sci. Technol. 46 (2012) 851–870.
[22] S. Woodward, R. Pearce, The role of stilbenes in resistance of sitka spruce (*Picea sitchensis* (Bong.) Carr.) to entry of fungal pathogens, Physiol. Mol. Plant Pathol. 33 (1988) 127–149.
[23] M. Lindberg, L. Lundgren, R. Gref, M. Johansson, Stilbenes and resin acids in relation to the penetration of *Heterobasidion annosum* through the bark of *Picea abies*, Eur. J. For. Pathol. 22 (1992) 95–106.
[24] S.G. Ralph, H. Yueh, M. Friedmann, D. Aeschliman, J.A. Zeznik, C.C. Nelson, Y.S. Butterfield, R. Kirkpatrick, J. Liu, S.J. Jones, M.A. Marra, C.J. Douglas, K. Ritland, J. Bohlmann, Conifer defence against insects: microarray gene expression profiling of sitka spruce (*Picea sitchensis*) induced by mechanical wounding or feeding by spruce budworms (*Choristoneura occidentalis*) or white pine weevils (*Pissodes strobi*) reveals large-scale changes of the host transcriptome, Plant Cell Environ. 29 (2006) 1545–1570.
[25] A.B. Groth, Investigations on Swedish turpentine, Svensk Papperstidning 60 (1958) 311–321.
[26] M. Lindmark-Henriksson, Biotransformations of turpentine constituents: oxygenation and esterification, Royal institute of technology, Stockholm (2003) 67 xii.
[27] Y. Yang, Z. Zhang, S. Li, X. Ye, X. Li, K. He, Synergy effects of herb extracts: pharmacokinetics and pharmacodynamic basis, Fitoterapia 92 (2014) 133–147.
[28] P.J. Delaquis, K. Stanich, B. Girard, G. Mazza, Antimicrobial activity of individual and mixed fractions of dill, cilantro, coriander and eucalyptus essential oils, Int. J. Food Microbiol. 74 (2002) 101–109.
[29] N. Valette, T. Perrot, R. Sormani, E. Gelhaye, M. Morel-Rouhier, Antifungal activities of wood extractives, Fungal Biol. Rev. 31 (2017) 113–123.
[30] G. Kleist, U. Schmitt, Characterisation of a Soft Rot-Like decay pattern caused by *Coniophora puteana* (Schum.) Karst. in sapelli wood (*Entandrophragma cylindricum* Sprague), Holzforschung (2001) 573.
[31] J.M. Toby, An algorithm for the construction of "D-Optimal" experimental designs, Technometrics 16 (1974) 203–210.
[32] L.Y. Chan, Optimal designs for experiments with mixtures: a survey, Commun. Stat. - Theory and Methods 29 (2000) 2281–2312.
[33] J. Palmer, Techniques and procedures for culturing ectomycorrhizal fungi, Mycorrhizae, Proceedings of the 1st North American Conference on Mycorrhizae, 1971, pp. 132–144.
[34] G.M. Eliopoulos, C.T. Eliopoulos, Antibiotic combinations: should they be tested? Clin. Microbiol. Rev. 1 (1988) 139–156.
[35] Z. Schelz, J. Molnar, J. Hohmann, Antimicrobial and antiplasmid activities of essential oils, Fitoterapia 77 (2006) 279–285.
[36] M. Nikkhah, M. Hashemi, M.B. Habibi Najafi, R. Farhoosh, Synergistic effects of some essential oils against fungal spoilage on pear fruit, Int. J. Food Microbiol. 257 (2017) 285–294.
[37] E. Kováts, Gas-chromatographische Charakterisierung organischer Verbindungen. Teil 1: Retentionsindices aliphatischer Halogenide, Alkohole, Aldehyde und Ketone, Helv. Chim. Acta 41 (1958) 1915–1932.
[38] H. Hotelling, Analysis of a complex of statistical variables into principal components, J Educ Psychol 24 (1933) 417–441.
[39] J. Trygg, S. Wold, Orthogonal projections to latent structures (O-PLS), J. Chemom., 16 (2002) 119–128.
[40] J. Trygg, O2-PLS for qualitative and quantitative analysis in multivariate calibration, J. Chemom. 16 (2002) 283–293.
[41] S. Wold, M. Sjöström, L. Eriksson, PLS-regression: a basic tool of chemometrics, Chemom. Intell. Lab. Syst. 58 (2001) 109–130.
[42] J. Maree, G. Kamatou, S. Gibbons, A. Viljoen, S. Van Vuuren, The application of GC–MS combined with chemometrics for the identification of antimicrobial compounds from selected commercial essential oils, Chemom. Intell. Lab. Syst. 130 (2014) 172–181.
[43] S. Burt, Essential oils: their antibacterial properties and potential applications in foods - A review, Int. J. Food Microbiol. 94 (2004) 223–253.
[44] F. Bakkali, S. Averbeck, D. Averbeck, M. Idaomar, Biological effects of essential oils – A review, Food and Chem. Toxicol. 46 (2008) 446–475.
[45] R. Shukla, P. Singh, B. Prakash, N.K. Dubey, Antifungal, aflatoxin inhibition and antioxidant activity of *Callistemon lanceolatus* (Sm.) Sweet essential oil and its major component 1,8-cineole against fungal isolates from chickpea seeds, Food Control 25 (2012) 27–33.
[46] J.G. Lopez-Reyes, D. Spadaro, A. Prelle, A. Garibaldi, M.L. Gullino, Efficacy of plant essential oils on postharvest control of rots caused by fungi on different stone fruits in vivo, J. Food Prot. 76 (2013) 631–639.
[47] I.H.N. Bassolé, H.R. Juliani, Essential oils in combination and their antimicrobial properties, Molecules 17 (2012) 3989.
[48] R. Kramer, W.R. Abraham, Volatile sesquiterpenes from fungi: what are they good for? Phytochem. Rev. 11 (2012) 15–37.
[49] T. Janah, M. Rahouti, A. Fidah, H.E.L. Houzali, B.E.L. Hallay, Y. Laadimi, M.R. Ismaili, M. Aberchane, A. Famiri, Chemical profiling and antifungal activity of essential oils of five moroccan threatened populations of cupressus atlantica gaussen, J. Essent. Oil-Bearing Plants 21 (2018) 1694–1705.
[50] D. Martin, D. Tholl, J. Gershenzon, J. Bohlmann, Methyl Jasmonate Induces Traumatic Resin Ducts, Terpenoid Resin Biosynthesis, and terpenoid accumulation in developing xylem of Norway spruce stems, Plant Physiol. 129 (2002) 1003–1018.
[51] S.-T. Chang, S.-Y. Wang, C.-L. Wu, P.-F. Chen, Y.-H. Kuo, Comparison of the antifungal activity of cadinane skeletal sesquiterpenoids from Taiwania (Taiwania cryptomerioides Hayata) Heartwood, Holzforschung (2000) 241.
[52] C.-L. Wu, S.-C. Chien, S.-Y. Wang, Y.-H. Kuo, S.-T. Chang, Structure-activity relationships of cadinane-type sesquiterpene derivatives against wood-decay fungi, Holzforschung (2005) 620.
[53] Y. Zhang, S. Muend, R. Rao, Dysregulation of ion homeostasis by antifungal agents, Front. Microbio. 3 (2012) 133.
[54] A. Ultee, M.H.J. Bennik, R. Moezelaar, The phenolic hydroxyl group of carvacrol is essential for action against the food-borne pathogen *Bacillus cereus*, Appl. Environ. Microbiol. 68 (2002) 1561–1568.
[55] T.L. Mason, W.P. Bruce, Inactivation of red beet β-glucan synthase by native and oxidized phenolic compounds, Phytochemistry 26 (1987) 2197–2202.